The observed evolution of oceanic pCO2 and its drivers over the last two decades

Andrew Lenton, Nicolas Metzl, Taro Takahashi, Mareva Kuchinke, Richard J. Matear, Tilla Roy, Stewart C. Sutherland, Colm Sweeney, Bronte Tilbrook

▶ **To cite this version:**

Andrew Lenton, Nicolas Metzl, Taro Takahashi, Mareva Kuchinke, Richard J. Matear, et al.. The observed evolution of oceanic pCO2 and its drivers over the last two decades. Global Biogeochemical Cycles, 2012, 26, pp.GB2021. 10.1029/2011GB004095 . hal-00753350

HAL Id: hal-00753350
https://hal.science/hal-00753350

Submitted on 4 Nov 2021

HAL is a multi-disciplinary open access archive for the deposit and dissemination of scientific research documents, whether they are published or not. The documents may come from teaching and research institutions in France or abroad, or from public or private research centers.

L'archive ouverte pluridisciplinaire **HAL**, est destinée au dépôt et à la diffusion de documents scientifiques de niveau recherche, publiés ou non, émanant des établissements d'enseignement et de recherche français ou étrangers, des laboratoires publics ou privés.

Copyright

The observed evolution of oceanic pCO_2 and its drivers over the last two decades

Andrew Lenton,[1] Nicolas Metzl,[2] Taro Takahashi,[3] Mareva Kuchinke,[1] Richard J. Matear,[1] Tilla Roy,[2] Stewart C. Sutherland,[3] Colm Sweeney,[4] and Bronte Tilbrook[1]

Received 20 April 2011; revised 2 April 2012; accepted 4 April 2012; published 19 May 2012.

[1] We use a database of more than 4.4 million observations of ocean pCO_2 to investigate oceanic pCO_2 growth rates. We use pCO_2 measurements, with corresponding sea surface temperature and salinity measurements, to reconstruct alkalinity and dissolved inorganic carbon to understand what is driving these growth rates in different ocean regions. If the oceanic pCO_2 growth rate is faster (slower) than the atmospheric CO_2 growth rate, the region can be interpreted as having a decreasing (increasing) atmospheric CO_2 uptake. Only the Western subpolar and subtropical North Pacific, and the Southern Ocean are found to have sufficient spatial and temporal observations to calculate the growth rates of oceanic pCO_2 in different seasons. Based on these regions, we find the strength of the ocean carbon sink has declined over the last two decades due to a combination of regional drivers (physical and biological). In the subpolar North Pacific reduced atmospheric CO_2 uptake in the summer is associated with changes in the biological production, while in the subtropical North Pacific enhanced uptake in winter is associated with enhanced biological production. In the Indian and Pacific sectors of the Southern Ocean a reduced winter atmospheric CO_2 uptake is associated with a positive SAM response. Conversely in the more stratified Atlantic Ocean sector enhanced summer uptake is associated with increased biological production and reduced vertical supply. We are not able to separate climate variability and change as the calculated growth rates are at the limit of detection and are associated with large uncertainties. Ongoing sustained observations of global oceanic pCO_2 and its drivers, including dissolved inorganic carbon and alkalinity, are key to detecting and understanding how the ocean carbon sink will evolve in future and what processes are driving this change.

Citation: Lenton, A., N. Metzl, T. Takahashi, M. Kuchinke, R. J. Matear, T. Roy, S. C. Sutherland, C. Sweeney, and B. Tilbrook (2012), The observed evolution of oceanic pCO_2 and its drivers over the last two decades, *Global Biogeochem. Cycles*, *26*, GB2021, doi:10.1029/2011GB004095.

1. Introduction

[2] Concentrations of atmospheric CO_2 continue to rise at unprecedented rates, reflecting continued carbon dioxide emissions [e.g., *Raupach et al.*, 2007]. The earth's oceans play a critical role in mitigating climate change by taking up more than 30% of the anthropogenic CO_2 emitted to the atmosphere [*Sabine et al.*, 2004a]. The oceans take up CO_2 primarily through air-sea gas exchange, which is a function (to a first order) of both the gas transfer coefficient and the difference between the partial pressures of seawater and the atmosphere (1).

$$\Delta pCO_2 = pCO_2^{OCEAN} - pCO_2^{ATMOSPHERE} \quad (1)$$

The growth rate of oceanic pCO_2 relative to the atmospheric CO_2 value provides information on the evolution of the strength of the sink or source of atmospheric CO_2 in time. A region with an oceanic pCO_2 growth rate faster than the atmospheric growth rate can be interpreted as a decreasing sink of atmospheric CO_2; conversely an oceanic pCO_2 growth rate less than the atmospheric rate can be interpreted as an increasing sink of atmospheric CO_2. These growth rates can reveal important information about the evolution of the ocean carbon sink.

[3] The change in oceanic surface pCO_2 (equation (2)) can be expressed as the sum of the changes in dissolved inorganic carbon (DIC), alkalinity (ALK), sea surface salinity (SSS) and sea surface temperature (SST), each of which responds to its own drivers and, hence, displays its own

[1]Wealth from Oceans Flagship, CSIRO Marine and Atmospheric Research, Hobart, Tasmania, Australia.
[2]LOCEAN-IPSL, CNRS, Université Pierre et Marie Curie, Paris, France.
[3]Lamont-Doherty Earth Observatory, Earth Institute at Columbia University, Palisades, New York, USA.
[4]Global Monitoring Division, ESRL, NOAA, Boulder, Colorado, USA.

Corresponding author: A. Lenton, Wealth from Oceans Flagship, CSIRO Marine and Atmospheric Research, Hobart, Tas 7004, Australia. (andrew.lenton@csiro.au)

Published in 2012 by the American Geophysical Union.

scales of variability. Consequently oceanic pCO_2 is highly variable in time and space [*Mahadevan et al.*, 2004]; and much of the variability in oceanic pCO_2 occurs on short timescales [*Lenton et al.*, 2006].

$$\begin{aligned} \mathrm{d}\ pCO_2/\mathrm{dt} = {} & (\partial pCO_2/\partial \mathrm{DIC})(\mathrm{d\ DIC/dt}) \\ & + (\partial pCO_2/\partial \mathrm{ALK})(\mathrm{d\ ALK/dt}) \\ & + (\partial pCO_2/\partial \mathrm{SSS})(\mathrm{d\ SSS/dt}) \\ & + (\partial pCO_2/\partial \mathrm{SST})(\mathrm{d\ SST/dt}) \end{aligned} \quad (2)$$

There are two major oceanic mechanisms that can drive oceanic pCO_2 growth rates to be either faster or slower than the atmospheric growth rate: (i) changes in the intensity of biological production through changes in DIC and ALK; and/or (ii) changes in ocean physics that can lead to changes in SST, SSS, DIC and ALK in the upper ocean. Given the spatial heterogeneity of biological production, identifying biologically driven changes in oceanic pCO_2 can be challenging.

[4] The surface ocean, in all but a few locations, remains significantly under-sampled spatially and temporally with respect to carbon [*Monteiro et al.*, 2010]. Given the paucity of sampling and the large spatial and temporal variability in oceanic pCO_2, identifying robust, secular growth rates in oceanic pCO_2 remains a difficult and important challenge [*Gruber*, 2009]. Nevertheless many recent studies have published growth rates of oceanic pCO_2 in different regions, and over different periods, from both time series and underway measured and calculated values of pCO_2. Next, we review these studies, indicating the temporal period over which changes have been calculated.

[5] Studies in recent decades have identified the high latitude Southern Ocean as a region where the oceanic pCO_2 growth rate is greater than that of the atmosphere, namely, *Metzl* [2009] (1991–2007) and *Takahashi et al.* [2009] (1984–2007), suggesting that the strength of the sink has decreased in recent decades both for the austral summer and winter. This decrease has been attributed to increased upwelling of carbon-rich deep-water associated with a strengthening Southern Annular Mode [e.g., *Le Quéré et al.*, 2007; *Lenton et al.*, 2009b; *Lenton and Matear*, 2007; *Lovenduski et al.*, 2007]. The decrease in Southern Ocean CO_2 uptake is mirrored by a decrease in CO_2 uptake in the North Atlantic sub-polar gyre [e.g., *Schuster et al.*, 2009; *Corbière et al.*, 2007; *Omar and Olsen*, 2006; *Metzl et al.*, 2010]. In contrast to the Southern Ocean, different mechanisms driving the changes in the North Atlantic have been proposed, including vertical [*Ullman et al.*, 2009] and horizontal physical processes [*Thomas et al.*, 2008]. Varying rates of pCO_2 change that have been reported in the North Atlantic may depend on the duration of time series used. Data series longer than about 25 years are needed to obtain a more reliable regional rate, which shows clearly the effect of drivers such as SST increase [*McKinley et al.*, 2011].

[6] The North Pacific oceanic pCO_2 growth rate has large spatial variability [*Takahashi et al.*, 2006]. The oceanic pCO_2 increase in the North Pacific subpolar gyre appears to be tracking the atmosphere for the period 1970 to 2004 [*Takahashi et al.*, 2006], unlike in other high-latitude regions. The areas encompassing the Bering and Okhostk Seas [*Takahashi et al.*, 2006] were the exception in this region with oceanic pCO_2 growth rates significantly less than that of the atmosphere. In these areas changes in oceanic pCO_2 growth rates were driven by the combination of enhanced biological production and changes in vertical mixing.

[7] Studies in the Northern and Southern sub-tropical gyre regions typically show that the oceanic pCO_2 growth rate is tracking the atmosphere in the North Atlantic [e.g., *Bates*, 2001, 2007; *Gruber et al.*, 2002; *Santana-Casiano et al.*, 2007]; in the North Pacific (1984–2006 [*Midorikawa et al.*, 2005; *Inoue et al.*, 1995] and 1970–2004 [*Takahashi et al.*, 2006, 2009]); in the South Pacific [*Takahashi et al.*, 2009] and Southern Indian [*Metzl*, 2009] (1991–2007). The exception to this sub-tropical pattern occurs at the Hawaii Ocean Time series site (HOTS) [*Dore et al.*, 2003; *Keeling et al.*, 2004], where the oceanic growth rate is faster than the atmospheric growth rate. However, as the studies at HOTS were based on limited spatial sampling, which may bias these results [*Takahashi et al.*, 2006].

[8] In the equatorial regions, with the exception of the Equatorial Pacific, very few studies have been published. The equatorial Pacific itself is a very complex region with large oceanic pCO_2 variability in response to the Pacific Decadal Oscillation and El Nino-La Nina events [*Feely et al.*, 2002]. The calculated growth rate of oceanic pCO_2 can be strongly biased by the observational period [*Feely et al.*, 2006]. However, *Feely et al.* [2006] (1981–2004), *Ishii et al.* [2009] (1980–2006), and *Takahashi et al.* [2009] (1974–2005) all estimate a mean oceanic pCO_2 growth rate close to the atmospheric value over the respective time scales.

[9] Despite the wealth of regional studies on changes in oceanic CO_2 uptake, synthesizing a synoptic global view and attributing the changes to processes remains highly challenging. These studies are often records of varying length and sampling density. Many of the published studies have also been based on pCO_2 measurements alone, and often do not have concomitant measurements of DIC and ALK making attribution to processes challenging. Nevertheless, a picture of the evolution of the global CO_2 sink appears to emerge. With the exception of the Western Pacific, there is a pattern of reduced CO_2 uptake at high latitudes, while oceanic pCO_2 in the low to midlatitudes oceans tends to track the atmospheric value. This is consistent with the results of a recent modeling study by *Le Quéré et al.* [2010], which identified that climate-driven changes, including strengthening winds and ocean warming, play a key role in the global air-to-sea CO_2 flux variations.

[10] An important recent development in ocean carbon science is the release of the LDEO_V2009 database [*Takahashi et al.*, 2009], which contains more than 4.4 million individual measurements of oceanic pCO_2 made since 1972. An earlier version of this database was used to construct global climatological values of ΔpCO_2 and maps of air-sea CO_2 flux [*Takahashi et al.*, 1997, 2009]. This allows changes in oceanic pCO_2 to be assessed in different ocean regions over the same period and also permits the estimation of seasonal changes in oceanic pCO_2. This can be significant as focusing on the multiyear annual (all-seasons) values alone, rather than values in different seasons (summer and winter), the changes in one season maybe compensated in another, leading to a biased view. In addition, understanding what is

driving these growth rates in different seasons is extremely important as it allows us to: (i) separate biological and physical changes in the ocean carbon cycle; (ii) identify the major drivers of change and use this to project how a changing climate may impact on ocean carbon uptake; and (iii) develop a way to assess and validate model simulations i.e., whether we are getting the right response for the right reasons in the historical period and to identify which process are key to future projections.

[11] In this study we are interested in probing what is driving the growth rates in oceanic pCO_2 in different regions. We utilize the LDEO_V2009 pCO_2 database [*Takahashi et al.*, 2009] to reconstruct the global fields of DIC and ALK. This reconstruction is assessed against all available upper ocean measurements of DIC and ALK to estimate the uncertainty in the reconstructed fields. We first investigate the longer-term growth rates during in all seasons, winter and summer. The reconstructed fields of ALK and DIC are then used, in conjunction with in situ temperature and salinity measurements, to investigate what is driving the oceanic pCO_2 response in different regions (see equation (2)). Finally, we investigate whether any large-scale global patterns of oceanic pCO_2 can be detected.

2. Methods

2.1. Calculation of Carbon Parameters

[12] To explore the evolution of the ocean carbon system we used the LDEO_V2009 database of oceanic pCO_2, which contains more than 4.4 million high-resolution measurements of pCO_2 collected since 1972 [*Takahashi et al.*, 2009]. Since we want to understand the drivers of oceanic pCO_2, we only use data with concomitant values of SST and SSS. This results in a reduction of about 15% ($\sim 6 \times 10^5$) in the size of the database. We first calculate values of alkalinity (ALK) and then values of dissolved inorganic carbon (DIC). In these calculations we first calculated DIC and ALK based on each triplet and then binned the data.

$$\mathrm{ALK} = \mathrm{a} + \mathrm{b}(\mathrm{SSS} - 35) + \mathrm{c}(\mathrm{SSS} - 35)^2 + \mathrm{d}(\mathrm{SST} - 20) + \mathrm{e}(\mathrm{SST} - 20)^2 \quad (3)$$

Two carbon parameters are needed to characterize the ocean carbonate chemistry. We have pCO_2 and estimated ALK calculated from sea surface temperature (SST) and sea surface salinity (SSS) according to *Lee et al.* [2006] (equation (3)). The relationship of *Lee et al.* [2006] is based on relationship between surfaces values of ALK, SST and SSS where the constants a–e are estimated from observations of five distinct oceanographic regions. To assess reconstructed fields we compared our annual mean fields of ALK between 1990 and 2008 with the gridded ALK from GLODAP [*Sabine et al.*, 2005]. The magnitude and the structure of reconstructed ALK agree well with GLODAP ALK (Figure 1) in all major ocean regions giving confidence in the relationships of *Lee et al.* [2006].

[13] The DIC values are calculated using the equations of carbonate chemistry from the reconstructed values of ALK and measured SST, SSS and pCO_2. Our implementation of carbonate chemistry is derived from the OCMIP3 framework (O. Aumont, C. Le Quéré, and J. C. Orr, NOCES Project Interannual HOWTO, 2004, available at http://www.ipsl.jussieu.fr/OCMIP/). The dissociation constants used in our calculations are from *Mehrbach et al.* [1973] refitted by *Dickson and Millero* [1987].

[14] We note that choice of another set of constants [e.g., *Lueker et al.*, 2000] would result in a change in the mean state and not significantly change the temporal gradient [*Corbière et al.*, 2007] and therefore not alter our conclusions significantly. As concomitant measurements of surface nutrients are not available within the LDEO_V2009 data set we choose to neglect the impact of nutrients on ALK, rather than to use climatology values that may bias the growth rates.

[15] Oceanic pCO_2 variability is dominated primarily by intraseasonal variability (i.e., eddy-scale variability) with temporal length scales typically ranging from a few days to months and spatial length scales ranging from tens of kilometers at high-latitudes to hundreds of kilometers in the equatorial regions [*Li et al.*, 2005]. To reduce the impact of mesoscale variability on each field, while retaining the oceanic structure, we averaged our SST, SSS, pCO_2, DIC and ALK data onto a $1^\circ \times 1^\circ$ monthly global grid. Additionally sampling studies of oceanic pCO_2 have shown that sampling at higher temporal frequencies than monthly do not return more information on the regional-scale response of the carbon system *Lenton et al.* [2006, 2009a] and *Takahashi and Sweeney* [2002].

[16] To ensure that we are only using open ocean data, thereby reducing the influence of heterogeneous coastal processes [e.g., *Chen and Borges*, 2009] on the region scale, we defined the coastal zone as having an ocean depth <200 m and removed all data in this zone from the data set. The bathymetry of the global ocean was taken from the ETOPO60 data set. After binning and filtering the data we are left with more than 75,000 independent measurements for which we have a value of pCO_2 and its constituent parts (equation (2)) i.e., SST, SSS, DIC and ALK.

[17] To assess the validity of our reconstruction we compiled all bottle data measurements of DIC and ALK available from the Carbon Dioxide Information Analysis Center (CDIAC) [*Key et al.*, 2004] and the recently released Carbon dioxide in the Atlantic Ocean (CARINA) database [*Key et al.*, 2010] for upper ocean samples (≤10 m depth). In most cases, these DIC and ALK values are from cruises with observed pCO_2, SSS and SST. We took the mean of the observed values in the 10 m surface layer and calculated a $1^\circ \times 1^\circ$ grid of monthly values and then compared these values with our calculated values on the same spatial and temporal grid. Values of DIC and ALK were only used when SST of the surface bottle samples agreed with underway SST values to within $\pm 0.25^\circ$C. The result was 3,900 comparison values or ~5% of the total calculated monthly values from pCO_2. Figure 2 shows the standard deviation ($1-\sigma$) of the zonal mean difference between observed and derived values, plotted as a function of latitude, for both DIC and ALK.

[18] We see good agreement in observed and calculated ALK and DIC for many regions, particularly in the Southern Ocean and Southern Hemisphere waters, excluding the data from 10°S to the equator off the coast of Southern America. Here, sparse sampling in the Equatorial Atlantic strongly biases the variance. We see that a large spike occurring 8°N

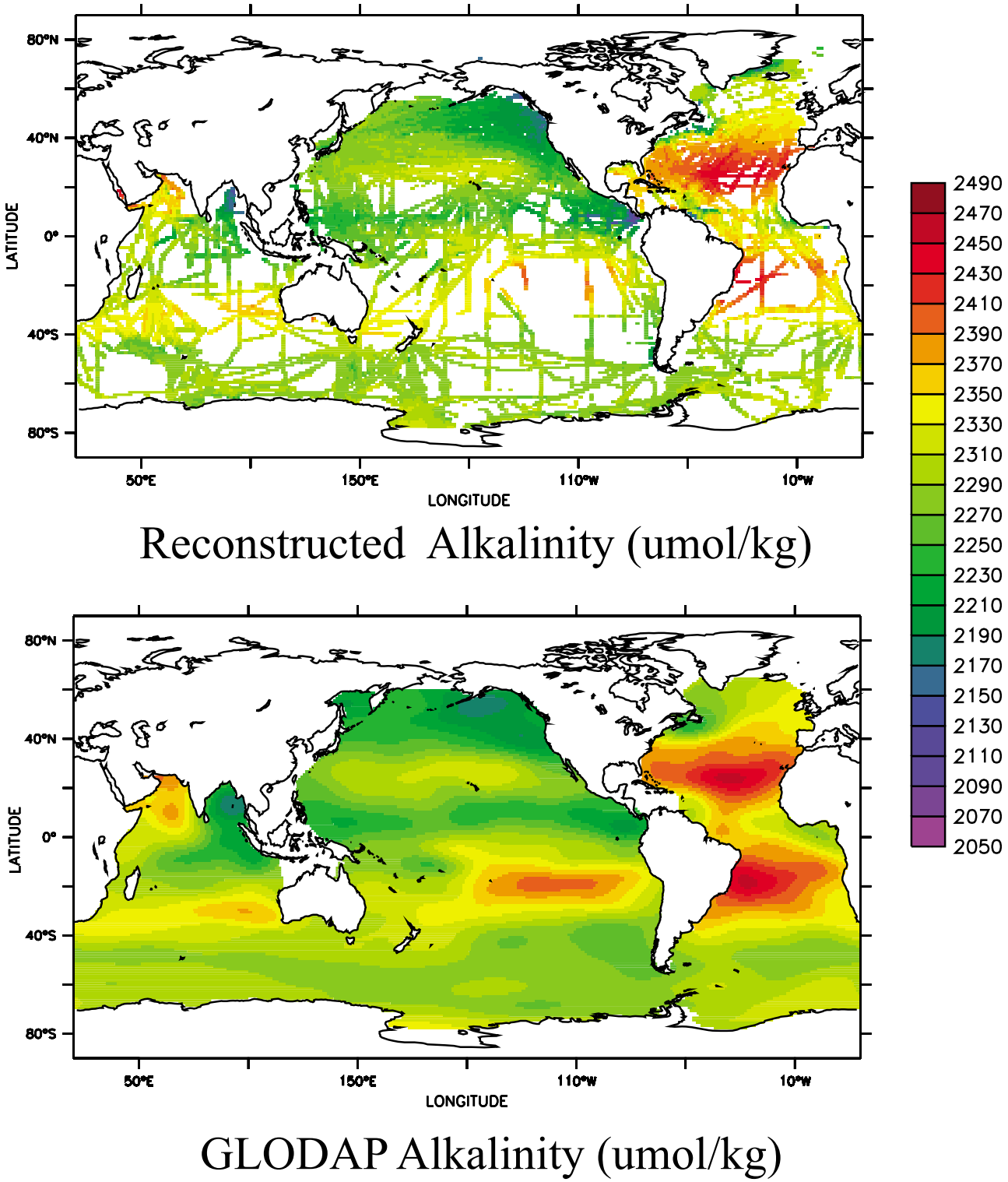

Figure 1. Comparison of the reconstructed mean alkalinity following *Lee et al.* [2006] in the period 1990–2008 and that from the gridded global GLODAP alkalinity fields [*Key et al.*, 2004].

is strongly influenced by the data from the Arabian Sea. The regions where observed and estimated ALK and DIC show a poor comparison generally represent poorly sampled regions or regions of upwelling. For the North Pacific, unfortunately very few observations of DIC and ALK are available in GLODAP or CARINA data sets for validation of the reconstructions.

[19] The accuracy of SST and SSS are both conservatively estimated to be 0.01°C and 0.01 salinity units. The level of uncertainty on pCO_2 is reported to be ± 2.5 μatm [*Takahashi et al.*, 2009]. When the large changes associated with the

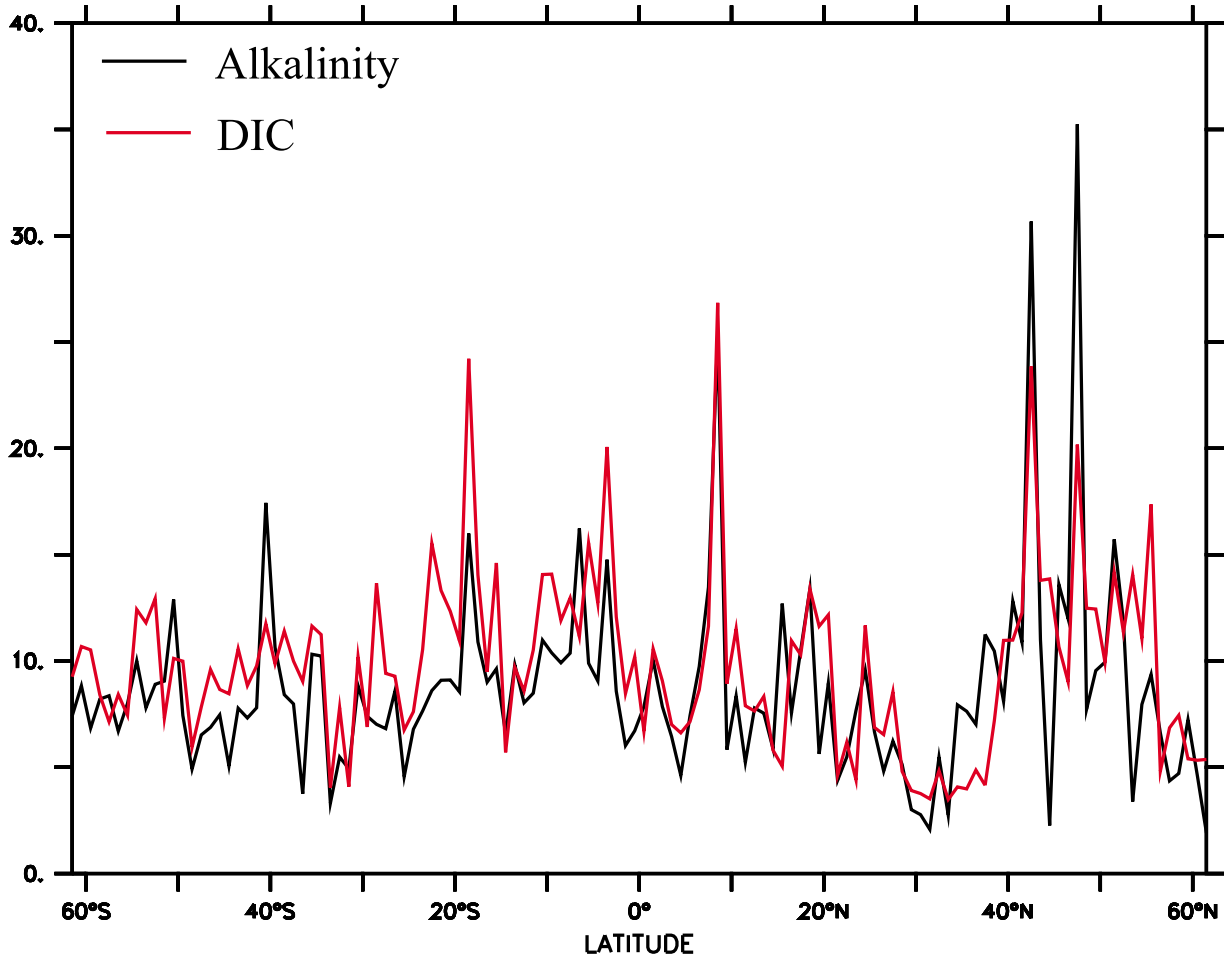

Figure 2. Zonal mean of the difference observed values (CDIAC and CARINA) and our reconstructed ALK (based on *Lee et al.* [2006]) and DIC derived from oceanic pCO_2 and ALK. Units are μmol kg^{-1}.

Equatorial Pacific and the Arabian Sea are removed, we estimate the global mean uncertainty of ALK to be ± 8 μmol kg^{-1} from Figure 2. This uncertainty in ALK was consistent with the uncertainty calculated by *Lee et al.* [2006], providing added confidence to our reconstruction. The corresponding uncertainty in DIC was estimated to be ± 9 μmol kg^{-1}. This error is slightly greater than but consistent with the uncertainty of ± 5–7 μmol kg^{-1} in the calculation of DIC by *Millero et al.* [1993] using a ± 4 μmol kg^{-1} error in ALK. Independently assessing the reconstructed fields of DIC and ALK allows us to treat these fields as independent of SSS and SST in all subsequent analyses.

2.2. Calculation of Regional pCO_2 Growth Rates

[20] For the regional analysis of pCO_2 growth rates, the ocean was partitioned into thirteen ocean regions, as listed in Table 1. In the high latitude Northern Hemisphere we selected latitudes that correspond to the southern boundary of the subpolar gyre. The Southern Ocean corresponds to the ocean between the subtropical front to the edge of the seasonal sea-ice zone. In the equatorial regions we chose the 10 degrees either side of the equator. Subtropical regions were defined as the region between the equatorial and subpolar regions. We did not calculate changes for the Arctic and the marginal seas around Antarctica due to limited observations. In each region we assessed the maximum and minimum SST and pCO_2 using Reynolds' observed SST products [*Reynolds et al.*, 2002] and the global monthly $4^\circ \times 5^\circ$ pCO_2 climatology of *Takahashi et al.* [2009] respectively. We also opted initially to separate the high-latitude

Table 1. The Latitude and Longitude of the Ocean Regions Used in This Study and the Period Over Which Growth Rates and Their Drivers Are Assessed

Region	Latitude	Longitude	Period
Western Subarctic North Pacific (SWNP)	42N–62N	129E–180E	1995–2003
Eastern North Pacific (ENP)	40N–62N	180E–120W	–
Subtropical North Pacific (STNP)	30N–42N	120E–105W	1996–2005
Equatorial Pacific (EqPac)	10N–10S	160W–70W	–
Subtropical South Pacific (STSP)	10S–45S	60W–10E	–
Subpolar North Atlantic (SNA)	40N–62N	68W–2W	–
Subtropical North Atlantic (STNA)	10–40N	80W–5W	–
Equatorial Atlantic (EqAtl)	10N–10s	120E–30W	–
Subtropical S. Atlantic (SSA)	10S–45S	60W–10E	–
North Indian (NIND)	10N–30N	10E–100E	–
Equatorial Indian (EqInd)	10N–10S	10E–100E	–
Subtropical South Indian (SIND)	10S–45S	10E–140E	–
Southern Ocean (SO)	45S–62S	Circumpol	1995–2008

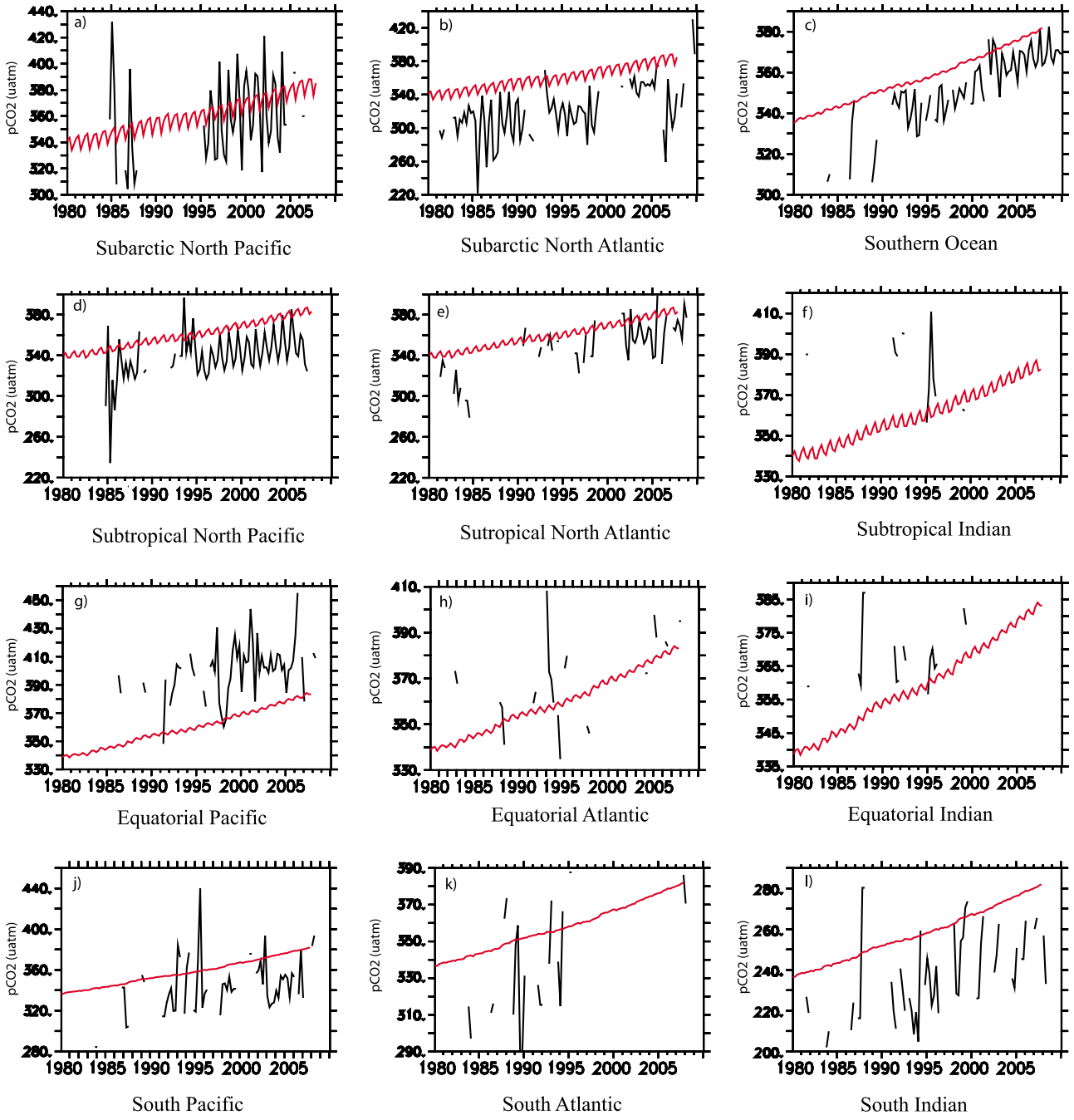

Figure 3. Monthly mean observed oceanic pCO_2 in different regions in the period 1980–2008. Overlain on each plot are the atmospheric CO_2 values (in red). Values below the atmospheric growth rate represent regions of ocean carbon uptake, while values above represent ocean sources.

North Pacific into Eastern and Western Hemispheres, following the analysis of *Takahashi et al.* [2006].

[21] Some regions (i.e., the Southern Ocean, the subarctic and the subtropical North Pacific) still had oceanic pCO_2 values that are much higher than expected within the open ocean—even after removing data in areas less than 200 m in depth (i.e., next to the coast). We interpreted this as 'contamination' of the open ocean with coastal data. These coastal values could potentially bias calculations of regional growth rates. To exclude this data, pCO_2 values exceeding two standard deviations from the regional mean were excluded.

[22] The temporal coverage of oceanic pCO_2 in all regions is shown in Figure 3. The regions that contain complete, or semi-complete, records from the mid 1990s onwards and have a well-represented seasonal cycle are: the Southern Ocean, the subarctic and subtropical North Pacific and the Equatorial Pacific allowing us to assess multidecadal changes in oceanic pCO_2 growth rate. The ocean carbon cycle variability in the Equatorial Pacific is strongly influenced by large-scale climate variability (such as the ENSO and the

Pacific Decadal Oscillation (PDO)) [*Feely et al.*, 2002]. Consequently, our ability to reconstruct ALK and DIC is poor and we have chosen not to include the Equatorial Pacific in our analysis. In the remaining regions there was insufficient coverage to assess the multidecadal variability i.e., a well-represented seasonal cycle over multiple decades.

2.3. Calculation of Oceanic and Atmospheric Growth Rates

[23] The detection of growth rates at the monthly scale is highly challenging due to variability in oceanic pCO_2 and under-sampling in most regions. Therefore, by binning the data into seasonal (3-month) mean values we reduce the intraseasonal variance and potential biases. We focus on changes in both summer and winter following *Metzl* [2009], and in all seasons (annual change). The January to March period is taken to be summer in the Northern Hemisphere and winter in the Southern Hemisphere. While, the July to September period is taken to be winter in the Southern Hemisphere and summer in the Northern Hemisphere.

[24] We use linear regression to calculate the growth rates in both the atmospheric and oceanic pCO_2 which assumes that the growth rate is linear, which is consistent with observational studies. Uncertainty in the oceanic pCO_2 growth rate and its drivers is calculated following *Wilks* [2006]. This error in the growth rate is significantly larger than the uncertainty associated with the binning of the observations. Therefore, we are confident that the uncertainty associated with the calculation of the growth rates is a very good approximation of the total error in the slope.

[25] Globally in the period 1995–2008 an atmospheric CO_2 growth rate of 1.9 μatm yr^{-1} (Seasonally $R^2 > 0.99$) was calculated. As the response is primarily linear we focus on the changes in physical and biological drivers of changes in pCO_2 growth rate rather than changes in atmospheric growth rate. The growth rate of atmospheric CO_2 was calculated from the monthly gridded (by latitude) CO_2 values from Globalview [*Earth System Research Laboratory*, 2009] and we assumed zonal homogeneity.

2.4. Determining Drivers of Oceanic pCO_2 Growth Rates

[26] We use linear regression to calculate the all season, winter and summer growth rates for each of the drivers of the oceanic pCO_2 growth rates (SSS, SSS, ALK, DIC). The relative contribution of the drivers to the pCO_2 growth rate were assessed by converting the growth rates of the drivers into pCO_2 units (μatm) using the approximations of *Takahashi et al.* [1993]. To calculate the Revelle factors for surface waters we used the approximations of *Sarmiento and Gruber* [2006], calculated using GLODAP DIC and ALK [*Key et al.*, 2004].

[27] In our analysis we focus on the changes in oceanic pCO_2 growth rate in response to changes in SSS (freshwater flux), biological production and ocean physics. To account for any changes in the hydrological cycle on carbon chemistry over the study period we normalize the values of ALK and DIC to 34.0 [*Chen and Millero*, 1979]. We recalculate the DIC and ALK growth rates based on the normalized ALK and DIC values (nDIC and nALK). The influence of biological production and ocean physics can be then teased apart by an analysis of the differences between the summer and winter nDIC and nALK growth rates. For example, in the high-latitudes the changes in the winter nDIC and nALK growth rates are largely a response to ocean physics. In the summer, the changes in the nDIC and nALK growth rates, relative to the winter, are a combined response to changes in biological production and ocean physics.

[28] The residuals between the summation of the drivers and the observed oceanic pCO_2 growth rate can be attributed to: i) the use of a spatial and temporal mean Revelle factor with no seasonality; ii) the a priori assumption that growth rates are linear; iii) the approximation of the change in oceanic pCO_2 by each individual component following *Takahashi et al.* [1993].

3. Results and Discussion

[29] In this section we present and discuss the oceanic pCO_2 growth rates for each region annually (all seasons), summer and winter. To assess the contribution of each of the drivers (ALK, DIC, SSS, SST) to the oceanic pCO_2 growth rate we calculate the growth rates of each of the drivers, which are presented in Tables 2–5. To quantify the contribution of each of these drivers to the oceanic pCO_2 growth rate we convert the growth rate of each of the drivers into units of pCO_2 (μatm), which are presented in Figures 4–7. Also, we present the time series of the seasonal data for each region in Figures S1–S4 in the auxiliary material.[1]

3.1. The Subarctic Western North Pacific

[30] In the subarctic North Pacific, sampling is strongly biased to the Western Hemisphere, and hence we focus on this region (42°N–50°N and 150°E–170°E). For the period 1995–2003, there is a coherent and well-defined seasonal cycle in all primary fields. The subarctic Western North Pacific is characterized by strong summer biological activity and winter vertical mixing supplying carbon and nutrients from the subsurface. The Western North Pacific is a net sink of atmospheric CO_2 [*Takahashi et al.*, 2009] with large multiyear variability (Figure 3).

[31] The increase of oceanic pCO_2 growth (1.6 ± 1.7 μatm yr^{-1}) is similar to the atmospheric CO_2 growth rate (1.9 μatm yr^{-1}) in all seasons, indicating that this region is tracking the atmosphere for the period 1995–2003 (Figure 4). Our calculated annual growth rate is in agreement with the observed value of 1.4 ± 0.8 μatm yr^{-1} reported by *Takahashi et al.* [2006] over the period 1970–2004. Our calculated values have a larger uncertainty than *Takahashi et al.* [2006], which may reflect the shorter length of our time series.

[32] The SST shows little change, however an SSS increase is evident (Table 2). This SSS increase is qualitatively consistent with the long-term increase in salinity observed in this region over the 1950–2000 period [*Durack and Wijffels*, 2010]. The values in DIC and ALK for all seasons (Table 2) both show large increases over the period (1995–2003). However, when we normalize DIC and ALK to salinity these increases are significantly reduced, suggesting that the observed increases in DIC and ALK are largely driven by the increases in SSS over the study period. Therefore we see that the oceanic pCO_2 growth rate is driven primarily by increases in DIC, offset by increases in ALK (Figure 4).

[1] Auxiliary materials are available in the HTML. doi:10.1029/2011GB004095.

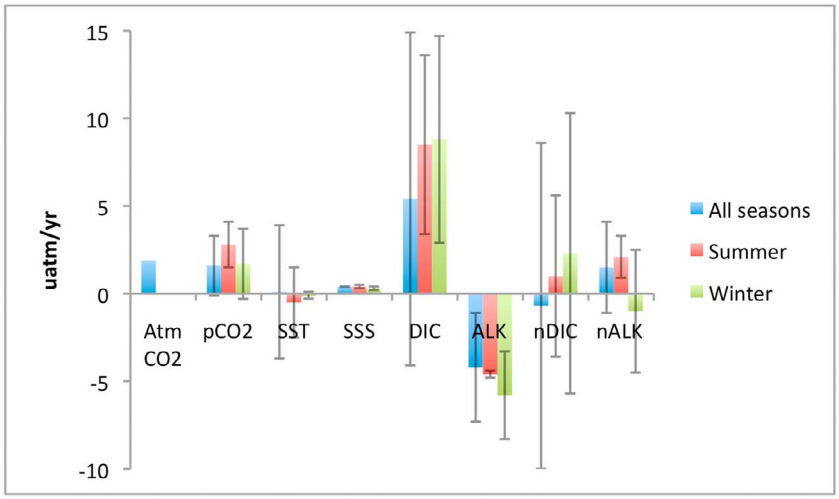

Figure 4. Summer, winter and all seasons (annual) CO_2 growth rates and their associated uncertainty in the Western Subpolar North Pacific over the period 1995–2003 in units of pCO_2. Illustrated are the atmospheric and oceanic growth rates, the drivers of oceanic pCO_2 and the growth rates of DIC and ALK normalized to constant salinity.

[33] The winter oceanic pCO_2 value (Figure 4) is close to the atmospheric CO_2 growth rate i.e., tracking the atmospheric CO_2 growth rate over the study period. The DIC, ALK and SSS all demonstrate strong increases, while SST shows a net decrease (Table 2). Analogous to the total response (all seasons) the winter oceanic pCO_2 growth rate can be explained by increases in DIC leading to increased pCO_2, with a strong compensating role played due to ALK (Figure 4).

[34] In winter, the normalization of DIC and ALK to constant salinity demonstrates that the strong positive growth rates in DIC and ALK can be explained by the observed SSS increases in the winter months (Table 2; nDIC and nALK). The increase in SSS, the decrease in SST and the similarity in the magnitude of nDIC to nALK growth rates suggest that vertical process play a key role in influencing the growth rates of DIC and ALK.

[35] The summer oceanic pCO_2 growth rate increases faster than the atmospheric CO_2 growth rate (Figure 4 and Table 2), in contrast to the winter. This suggests that the strength of the summer CO_2 sink may be decreasing over the period 1995–2003 although this growth rate is associated with a large uncertainty. Analogous to the winter, DIC, ALK and SSS all show increases, while SST shows a decrease (Table 2). The faster oceanic pCO_2 growth rate in the summer relative to the winter growth rate is driven primarily by the difference between the growth rates of DIC and ALK (Figure 4 and Table 2).

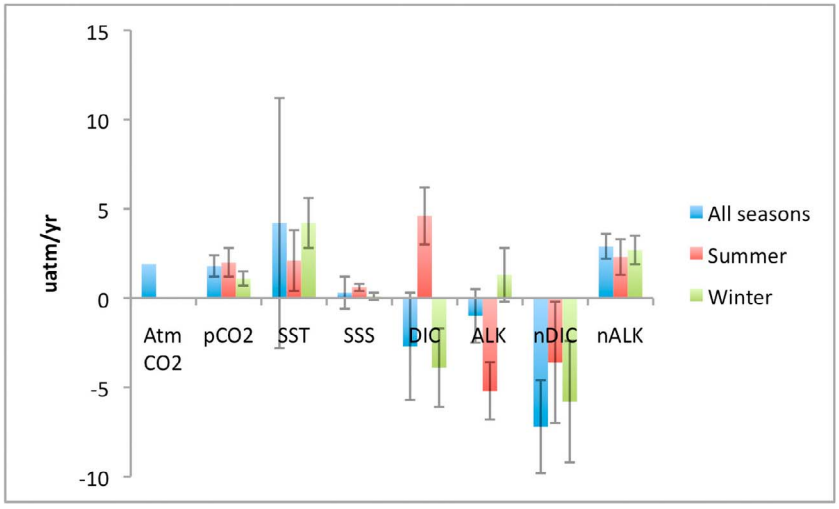

Figure 5. Summer, winter and all seasons (annual) CO_2 growth rates and their associated uncertainty in the Subtropical North Pacific over the period 1996–2005 in units of pCO_2. Illustrated are the atmospheric and oceanic growth rates, the drivers of oceanic pCO_2 and the growth rates of DIC and ALK normalized to constant salinity.

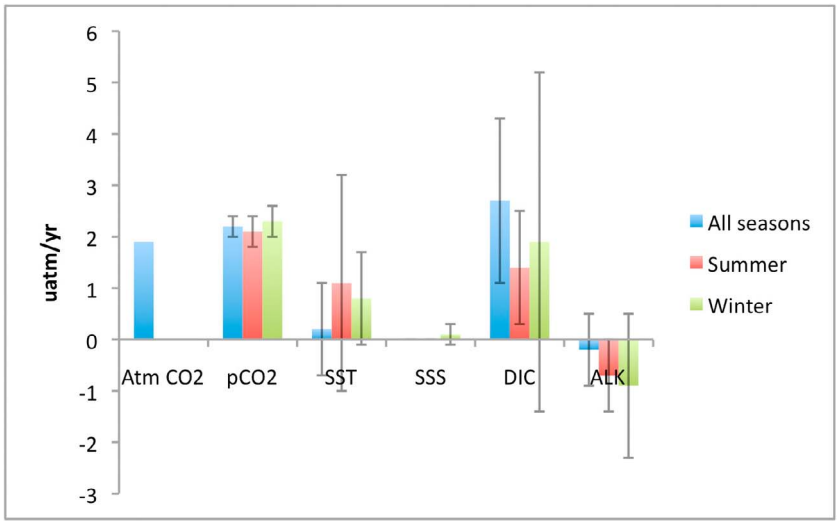

Figure 6. Summer, winter and all seasons (annual) CO_2 growth rates and their associated uncertainty in Indian and Pacific sectors of the Southern Ocean over the period 1995–2008 in units of pCO_2. Illustrated are the atmospheric and oceanic growth rates, the drivers of oceanic pCO_2.

[36] When DIC and ALK are normalized to constant salinity we see large decreases in DIC and ALK growth rates, highlighting the strong impact of changes in SSS over the study period, which is consistent with the winter. The summer nDIC and nALK growth rates are less than the winter growth rates, suggesting an increase in biological production, which is consistent with observed changes over the study period from *Behrenfeld et al.* [2006] and *Gregg et al.* [2005]. Further, that the change in the nDIC:nALK growth rate ratio from winter to summer is close to 1:2, which strongly suggests that these biological changes may be attributable to an increase in $CaCO_3$ production.

[37] Our calculated summer DIC growth rate (3.3 ± 2.0 μmol kg^{-1} yr^{-1}; Table 2) is higher than the values reported in the greater Western North Pacific of 1.3 ± 2 μmol kg^{-1} yr^{-1} by *Feely et al.* [2003] and *Sabine et al.* [2004b] (1972–2003) based on non-winter months, although large uncertainty exists within all of these calculated growth rates. Nevertheless, these differences in the mean values may be explained by changes in SSS.

[38] Despite the large changes in the summer and winter values of DIC and ALK that occur in response to changes in salinity, this has little net impact on the oceanic pCO_2 growth rate. This is because in this region the oceanic growth rate is set primarily by ratio between the growth rates of DIC and ALK. As the ratio of the DIC to ALK growth rate remains unchanged with dilution, the net impact on

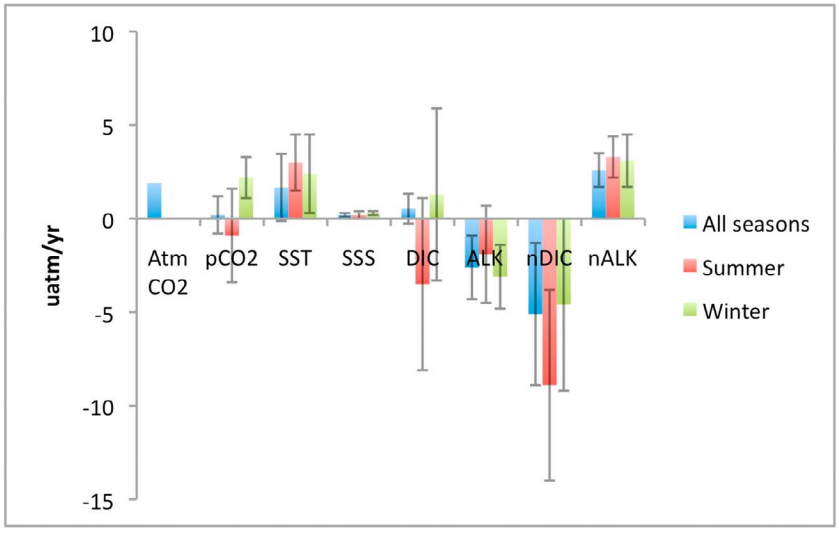

Figure 7. Summer, winter and all seasons (annual) CO_2 growth rates and their associated uncertainty in Atlantic sectors of the Southern Ocean over the period 2001–2008 in units of pCO_2. Illustrated are the atmospheric and oceanic growth rates, the drivers of oceanic pCO_2 and the growth rates of DIC and ALK normalized to constant salinity.

Table 2. Subarctic Western North Pacific Growth Rates and Uncertainty in Oceanic pCO_2 and Drivers Calculated in the Period 1995–2003

	Annual	Winter	Summer
pCO_2sw (μatm yr^{-1})	1.6 ± 1.7	1.7 ± 2	2.8 ± 1.3
SST (°C yr^{-1})	0.01 ± 0.25	−0.06 ± 0.11	−0.03 ± 0.13
SSS (units yr^{-1})	0.04 ± 0.01	0.03 ± 0.01	0.04 ± 0.01
DIC (μmol kg^{-1} yr^{-1})	2.1 ± 3.7	3.4 ± 2.3	3.3 ± 2.0
nDIC (μmol kg^{-1} yr^{-1})	−0.3 ± 3.6	1.3 ± 3.1	0.4 ± 1.8
ALK (μmol kg^{-1} yr^{-1})	2.0 ± 1.5	2.8 ± 1.2	2.2 ± 0.1
nALK (μmol kg^{-1} yr^{-1})	−0.7 ± 1.3	0.5 ± 1.7	−1.0 ± 0.6

oceanic pCO_2 growth rate from changes in the SSS, and pCO_2 directly, is very small over the study period.

3.2. Subtropical North Pacific

[39] The Subtropical North Pacific (STNP: 10°N–42°N) encompasses a very large surface area; hence the ranges in both SST and SSS are large. As this database is spatially biased to the northern part of the STNP we consider only data in the region 30°N–42°N, and in the period 1996–2005. We note in investigating this region that it is strongly influenced by the Pacific Decadal Oscillation (PDO) which can have a large impact on ocean carbon uptake [*Feely et al.*, 2002] in both its positive and negative phase. The STNP is oligotrophic and shows a large seasonal variability in CO_2: strong CO_2 drawdown occurs during the boreal winter in response to cooling and enhanced mixing, and reduced CO_2 uptake occurs in the summer due to warming [*Takahashi et al.*, 2009] (Figure 3).

[40] The STNP oceanic annual pCO_2 growth rate (1.8 ± 0.6 μatm yr^{-1}) appears to be tracking the annual atmospheric growth rate (1.9 μatm yr^{-1}) over the period 1996–2005. This is in good agreement with *Takahashi et al.* [2006], who found that the annual oceanic pCO2 growth rate was indistinguishable from the atmospheric growth rate over the period 1970–2004. The total increase (all seasons) seen in SST for the STNP (Table 3) is broadly consistent with observations of SST by *Gregg et al.* [2005] and *Polovina et al.* [2008] over the 1996–2005 period. An increase in SSS (Table 3) was also evident, which is also broadly consistent with the increases observed by *Durack and Wijffels* [2010].

[41] A net decrease in DIC and corresponding net increase in ALK (Table 3) is also present over the study period. A key driver of the total growth rate in oceanic pCO_2 in this region is SST acting to increase oceanic pCO_2, with decreases in DIC and increases in ALK playing a compensating role, acting together to reduce oceanic pCO_2 (Figure 5). When DIC and ALK are normalized to constant salinity we see large net decreases in DIC and ALK. Such large decreases could be explained through strong increases in biological production in response to a warmer ocean or a reduction in the strength of the winter upwelling (discussed later).

[42] During winter we see that the oceanic pCO_2 growth rate (1.1 ± 0.4 μatm yr^{-1}) is less than the atmospheric growth rate of 1.9 μatm yr^{-1}. This suggests that this region is an increasing sink of atmospheric CO_2 in the winter 1996–2005 period. Our winter oceanic pCO_2 growth rate is lower than that of *Inoue et al.* [1995] (i.e., 1.8 ± 0.6 μatm yr^{-1}) for the Western Pacific region (15°N–35°N) between 1984 and 1993. This lower value may reflect both the differences in spatial regions, and/or the differences in the atmospheric growth rate between the two periods.

[43] In the winter, increases in SST and SSS are associated with a net reduction in both DIC and ALK (Figure 5). It is this decrease in DIC that acts to enhance the oceanic uptake of atmospheric CO_2, while the increase in SST and the decrease in ALK play a compensating role and modulate the uptake. When DIC and ALK are normalized to constant salinity we see large net decreases in DIC and ALK, over the study period (Table 3).

[44] During the winter the oceanic pCO_2 growth rates appear to be a complex response to both biological production and changes in vertical supply. When DIC and ALK are normalized to constant salinity we see net decreases in nDIC and nALK growth rates. This coupled with the increases in SST suggest reduced vertical supply. This is consistent with studies that show an increase in stratification in this region and an expansion of the size of the oligotrophic gyres over this period [e.g., *Polovina et al.*, 2008]. Also, the increase in SST, in conjunction with the faster growth rates of nDIC than nALK, suggest that either there may have been enhanced production of organic carbon and/or changes in $CaCO_3$ production in response to a warmer ocean. This increase in production is consistent with *Gregg et al.* [2005] and *Behrenfeld et al.* [2006] who showed an increase in remotely sensed chlorophyll in the region 30°N–42°N over the periods 1998–2003 and 1999–2004 respectively.

[45] In the summer, we see that the oceanic pCO_2 growth rate (2.0 ± 0.8 μatm yr^{-1}) is similar to the atmospheric CO_2 growth rate over the study period (Figure 5). This suggests that the strength of the summer drawdown of atmospheric CO_2 is not changing. While we do see increases in SSS and SST consistent with the total response (all seasons) and winter, we also observe strong positive growth rates in DIC and ALK (Figure 5). Here, increases in DIC and SST act in concert to increase the oceanic pCO_2 growth rate and are compensated by increases in ALK (Figure 5). The ALK and DIC growth rates increase by the same magnitude from winter to summer (~4 μmol kg^{-1} yr^{-1}), this suggests that changes in winter biological production plays a key role in setting summer pCO_2 growth rates. The strong negative trends in nDIC and nALK suggest increased vertical stratification, consistent with the winter.

[46] The summer growth rates in DIC of 2.3 ± 0.8 μmol kg^{-1} yr^{-1} (Table 3) are larger than those of *Sabine et al.* [2008] and *Feely et al.* [2003] for the non-winter mixed

Table 3. Western Subtropical North Pacific Growth Rates and Uncertainty in Oceanic pCO_2 and Drivers Calculated in the Period 1995–2005

	Ann.	Winter	Summer
pCO2sw (μatm yr^{-1})	1.8 ± 0.6	1.1 ± 0.4	2.0 ± 0.8
SST (°C yr^{-1})	0.3 ± 0.5	0.2 ± 0.1	0.2 ± 0.1
SSS (units yr^{-1})	0.04 ± 0.1	0.01 ± 0.02	0.07 ± 0.02
DIC (μmol kg^{-1} yr^{-1})	−1.3 ± 1.5	−2.0 ± 1.1	2.3 ± 0.8
nDIC (μmol kg^{-1} yr^{-1})	−3.6 ± 1.3	−2.9 ± 1.7	−1.8 ± 1.7
ALK (μmol kg^{-1} yr^{-1})	0.6 ± 0.9	−0.8 ± 0.9	3.2 ± 1.0
nALK (μmol kg^{-1} yr^{-1})	−1.8 ± 0.4	−1.7 ± 0.7	−1.4 ± 0.6

Table 4. Southern Ocean Indian and Pacific Ocean Region Growth Rates and Uncertainty in Oceanic pCO_2 and Drivers Calculated in the Period 1995–2008

	Annual	Winter	Summer
pCO2sw (μatm yr^{-1})	2.2 ± 0.2	2.3 ± 0.3	2.1 ± 0.3
SST (°C yr^{-1})	0.01 ± 0.06	0.05 ± 0.06	0.07 ± 0.14
SSS (units yr^{-1})	0	0.01 ± 0.02	0
DIC (μmol kg^{-1} yr^{-1})	1.0 ± 0.6	0.7 ± 1.2	0.3 ± 0.4
ALK (μmol kg^{-1} yr^{-1})	0.1 ± 0.3	0.4 ± 0.6	0.3 ± 0.3

layer (1.3 ± 0.2 μmol kg^{-1} yr^{-1}; 1973–2000). While these differences may in part be explained by different atmospheric growth rates, they are more likely associated with the physical changes that have occurred over the two periods. A decrease in vertical supply would also account for the differences between our annual negative growth rate in DIC (−1.3 ± 1.5 μmol yr^{-1}) and the small positive growth rate of *Takahashi et al.* [2006] (0.6 ± 0.3 μmol yr^{-1}) in the mixed layer (1970–2004).

3.3. The Southern Ocean

[47] The Southern Ocean (45°S–62°S) still remains one of the ocean regions that is most under-sampled for carbon. The Southern Ocean acts as a key net annual sink of atmospheric CO_2 [*Takahashi et al.*, 2009] (Figure 3). This region has a high-nutrient low chlorophyll (HNLC) regime, characterized by strong vertical mixing that supplies nutrients and CO_2 to the surface during winter and by active photosynthetic utilization during summer [e.g., *Metzl et al.*, 2006].

[48] In our preliminary analysis for the period 1995–2008, we first estimate the total (all seasons) pCO_2 growth rate at 2.3 ± 0.2 μatm yr^{-1}, which is faster than the corresponding atmospheric growth rate of 1.9 μatm yr^{-1}. In summer, the calculated oceanic pCO_2 growth rate of 2.1 ± 0.3 μatm yr^{-1} is close to the atmospheric CO_2 growth over the same period, while in the winter months (where much less data is available), we calculated an oceanic pCO_2 of 2.5 ± 0.7 μatm yr^{-1}, close to the value of 2.2 ± 0.5 μatm yr^{-1} calculated by *Takahashi et al.* [2009] in the circumpolar ocean in the period 1983–2008, but not significantly different to the atmospheric growth rate of 1.9 μatm yr^{-1}. However, when we investigated the growth rates and drivers of oceanic pCO_2 they appear to vary significantly across the different ocean regions of the Southern Ocean. As shown later, since the growth rates and drivers in the Indian and Pacific Regions (0:295E) of the Southern Ocean are similar we combined these and considered the Atlantic Region (65W:0) separately.

3.3.1. The Indian and Pacific Sectors of the Southern Ocean

[49] In the Indian and Pacific sectors of the Southern Ocean (0:295E) 1995–2008, the annual growth rate in oceanic pCO_2 is 2.2 ± 0.2 μatm yr^{-1} (Figure 6 and Table 4), which is slightly larger than the annual ocean CO_2 growth rate over the same period. This suggests that annually this region is a very weakly decreasing sink of atmospheric CO_2. This is in good agreement with *Metzl* [2009] who calculated an annual pCO_2 growth rate of 2.4 ± 0.2 μatm yr^{-1} (1991–2007) for the Southwestern Indian Ocean.

[50] We see that there is no evidence of long-term growth rates in SST, SSS or ALK (Table 4 and Figure 6). The growth rate in oceanic pCO_2 is driven by the increase in DIC over the study period. An oceanic pCO_2 growth that is faster than the atmosphere growth rate, and driven primarily by DIC, is very consistent with the expected response to the positive phase of the Southern Annular Mode (SAM) [*Lenton et al.*, 2009b]. In its positive phase the SAM drives enhanced upwelling of carbon-rich deep water at high latitudes in response to enhanced poleward winds over the Southern Ocean, leading to an increase in the value of DIC and a subsequent reduction in atmospheric CO_2 uptake.

[51] In the winter, the oceanic pCO_2 growth rate (2.3 ± 0.3 μatm yr^{-1}) is above the atmospheric CO_2 growth rate: the region is acting is a weak decreasing sink of atmospheric CO_2 (Figure 6). This oceanic pCO_2 growth rate is in good agreement with the results of *Metzl* [2009] in the South-Western Indian Ocean, who calculated an annual pCO_2 growth rate of 2.1 ± 0.2 μatm yr^{-1} (1991–2000; 50–55S). In the winter, we see increases in SST, DIC and ALK (Table 4) over the study period. We see that the oceanic pCO_2 growth rate is dominated by increases in DIC with the increase in ALK balancing the increase in SST. These increases in DIC and ALK are consistent with the enhanced ventilation of carbon and nutrient rich deep waters associated with the SAM.

[52] In the summer we see that the oceanic pCO_2 growth rate (2.1 ± 0.3 μatm yr^{-1}; Figure 6 and Table 4) is similar to the atmospheric CO_2 growth rate. This is less than the growth rate of *Metzl* [2009] in the South-Western Indian Ocean, who calculated an annual pCO_2 growth rate of 2.4 ± 0.2 μatm yr^{-1} (1991–2000; 50–55S). This difference may reflect the selection of different regions in these studies. Increases in SST, DIC and ALK all occur over the summer periods. The pCO_2 growth rates are driven by the combination of increased DIC and SST, which is offset by increases in ALK (Figure 4). The lower summer DIC and ALK growth rates relative to the winter, and the increase SST, suggests that biological production may have increased over the recent decades. An increase in summer primary productivity in response to a strengthening SAM has been observed [*Lovenduski and Gruber*, 2005]. Interestingly however this does lead to an enhanced export production [*Lenton et al.*, 2009a].

[53] Observationally we see that strength of the SAM appears stronger in the 1990s than the 2000s (http://www.antarctica.ac.uk/met/gjma/sam.html). We see that pCO_2 growth rates are larger when calculated over the shorter period (i.e., 1995–2002) than when calculated over the entire observational period (i.e., 1995–2008).

3.3.2. The Atlantic Sector of the Southern Ocean Region

[54] Annually in the Atlantic Sector of the Southern Ocean we see little or no growth rate in oceanic pCO_2 (0.2 ± 1.0 μatm yr^{-1}) (Table 5 and Figure 7). Therefore this sector acts as an increasing net sink of atmospheric CO_2 over the period 2001–2008. Inspection of the drivers of annual (all seasons) oceanic pCO_2 growth rates (Figure 7 and Table 5) illustrates that the increasing sink is driven by the increases in DIC and SST growth rates, and is strongly compensated by the increase in ALK. Annually, when DIC and ALK are normalized to constant salinity, the growth rates in both

Table 5. Southern Ocean Atlantic Ocean Growth Rates and Uncertainty in Oceanic pCO_2 and Drivers Calculated in the Period 2001–2008

	Annual	Winter	Summer
pCO2sw (μatm yr^{-1})	0.2 ± 1.0	2.2 ± 1.1	−0.9 ± 2.5
SST (°C yr^{-1})	0.11 ± 0.12	0.16 ± 0.14	0.2 ± 0.1
SSS (units yr^{-1})	0.02 ± 0.01	0.03 ± 0.01	0.03 ± 0.02
DIC (μmol kg^{-1} yr^{-1})	0.2 ± 0.3	0.5 ± 1.7	−1.3 ± 1.7
nDIC (μmol kg^{-1} yr^{-1})	−1.9 ± 1.4	−1.7 ± 1.7	−3.3 ± 1.9
ALK (μmol kg^{-1} yr^{-1})	0.9 ± 0.7	0.9 ± 0.7	0.8 ± 1.1
nALK (μmol kg^{-1} yr^{-1})	−1.1 ± 0.4	−1.3 ± 0.6	−1.4 ± 0.5

nDIC and nALK (Figure 7 and Table 5) are strongly decreased. The strong decreases in nDIC and nALK could be explained by changes in stratification, which reduce vertical supply, and/or by enhanced biological production (discussed later).

[55] In winter, the oceanic pCO_2 growth rate (2.2 ± 1.1 μatm yr^{-1}) is close to the atmospheric pCO_2 growth rate, suggesting that this region is close to, but slightly above, the atmospheric CO_2 growth rate. However, it must be noted that there is a large uncertainty associated with this change. The oceanic pCO_2 growth rate can be explained by the balance between increased oceanic pCO_2, in response to increased SST and DIC, offset by an increase in ALK over the study period. When we normalize DIC and ALK to constant salinity we see that the nDIC and nALK growth rates are much less than DIC and ALK. This reduction coupled with an increase in SST can be explained by a reduction in the strength of the winter upwelling in this region.

[56] The summer oceanic pCO_2 growth rate (−0.9 ± 2.5 μatm yr^{-1}) is much less than the atmospheric growth rate (1.9 μatm yr^{-1}), suggesting that this region is acting as an increasing sink of atmospheric CO_2, even after accounting for the large uncertainty associated with these growth rate (Figure 7 and Table 5). In summer we see increases in SST and ALK consistent with winter, however there is a net decrease in DIC (Figure 7 and Table 5). The net oceanic pCO_2 growth rate can be explained by the reduction in DIC and the increase in ALK that is, in part, compensated by increases in SSS and SST. When we normalize DIC and ALK we see large decreases in the nDIC growth and little change in nALK growth rate from winter to summer suggesting large increases biological production (non-calcifying) over the study period. This is consistent with the hypothesis that increased stratification leads to enhanced summer biological production in the Southern Ocean [*Bopp et al.*, 2001].

3.3.3. Reconciling the Southern Ocean Responses

[57] Across the circumpolar Southern Ocean the winter oceanic pCO_2 growth rate is greater than the atmospheric CO_2 growth rate, which is consistent with *Takahashi et al.* [2009]. Our results, however, indicate that different mechanisms are influencing the surface ocean pCO_2 growth rate in the Atlantic and Pacific-Indian sectors. These mechanisms can be explained by the observed spatial structure of ocean stratification [*Dong et al.*, 2008]. Therefore we suggest that the SAM continues to plays a key role in driving the circumpolar Southern Ocean response through the ventilation of the carbon rich deep water. But, in the Atlantic sector vertical stratification dominates this ventilation response, leading to a net reduction in the supply of carbon rich deepwater.

4. Conclusion

[58] We used the global LDEO database (V2009), containing more than 4.4 million sea surface ocean pCO_2 observations collected over more than 35 years (1972–2008), to investigate the multiyear growth rates of oceanic pCO_2 growth rates and the drivers of these growth rates at the region scale. Alkalinity (ALK) was reconstructed following *Lee et al.* [2006] using relationships based on sea surface temperature and salinity. Dissolved inorganic carbon (DIC) was calculated from equilibrium carbonate chemistry. The values of DIC and ALK were then compared with concomitant values of DIC and ALK measured from upper ocean bottle data (≤10 m; CARINA and CDIAC). This comparison shows good agreement in most regions, and from this we estimate the global uncertainty in ALK to be ±8 μmol kg^{-1} and ±9 μmol kg^{-1} in DIC.

[59] As much of the global ocean remains under-sampled with respect to ocean carbon measurements, we averaged the data in each of the major ocean regions into seasonal bins to dampen high-frequency spatial and temporal variability. In the period 1995–2008 three regions had sufficient coverage in time and space to determine growth rates: the Subarctic Western North Pacific; Subtropical North Pacific; and the Southern Ocean. Despite adequate coverage, the Equatorial Pacific was excluded from the analysis due to a poor reconstruction of DIC and ALK fields and inherent large interannual variability in this region making it difficult to extract growth rates. In regions with sufficient data, the seasonal and annual growth rates (i.e., growth rates in all seasons) of oceanic pCO_2 and records of atmospheric CO_2 were used to assess whether the region acts as an increasing sink or source of atmospheric CO_2.

[60] In the Western Subpolar North Pacific we find that annually, and in the winter, the oceanic CO_2 growth rate appears to be tracking the atmosphere, while in the summer the oceanic pCO_2 growth rate is faster than the atmosphere, thus causing a reduction in the ocean's sink strength. This reduction in the summer is primarily due to increases in biological production, potentially marine calcifiers as indicated by the decrease in the salinity-normalized ALK. In the Subtropical North Pacific we see that in the summer, and annually, the oceanic pCO_2 growth rate is close to the atmosphere. However, in the winter the oceanic pCO_2 growth rate is exceeded by the atmospheric growth rate. This implies that this region acts as an increasing sink of atmospheric CO_2; driven primarily by enhanced biological production over the study period.

[61] In the Southern Ocean we see two distinct responses in the summer oceanic pCO_2 growth rates that are related to the differences in stratification between two sectors of the Southern Ocean. In the less stratified Indian and Pacific sector the oceanic pCO_2 growth rate is very close to the atmospheric CO_2 growth rate. However, in the more stratified Atlantic sector of the Southern Ocean the oceanic pCO_2 growth rate in the summer (and annually) is significantly less than the atmospheric CO_2 growth rate. Therefore in this sector we see a strongly enhanced sink of atmospheric CO_2 driven by enhanced biological production and vertical

stratification. In the winter in all sectors we see that the oceanic pCO_2 growth rate is faster than the atmospheric growth rate, suggesting that this region is acting as a reducing sink of atmospheric CO_2.

[62] Over the regions for which trends can be estimated, we see a net reduction in the strength of the global ocean sink in recent decades. We demonstrate that a regionally distinct set of mechanisms drive the changes in the oceanic pCO_2 growth rate in each region. We highlight the importance of investigating both the oceanic pCO_2 growth rates and its drivers at the seasonal scale rather than annually, which can strongly bias our detection and understanding of change at the region scale. We see that it is primarily the changes in DIC that are driving the changes in oceanic pCO_2 growth rate. In interpreting how this DIC growth rate drives the oceanic pCO_2 growth rate we have attributed the DIC growth rate to changes in ocean physics, freshwater fluxes and biological production.

[63] The air-sea CO_2 flux also contributes to changes in oceanic pCO_2 growth rates, however this is very difficult to assess observationally. If we account for these air-sea CO_2 fluxes we would underestimate the contribution of biological production and ocean physics to the oceanic pCO_2 growth rates. For example, in the majority of regions the atmospheric growth is slower than the oceanic pCO_2 growth rate and the DIC growth rates are positive. Here, the air-sea CO_2 flux would drive atmospheric CO_2 out of the ocean. Hence if we could remove the contribution of the air-sea CO_2 flux to the oceanic pCO_2 growth rate, the DIC growth rate would be enhanced. Therefore, our results suggest that the observed decline in the strength of the ocean carbon sink is driven by changes in ocean physics and biological processes.

[64] Interestingly, the recent observed changes SST and SSS appear to play an important role in setting the character of the ocean carbon sinks through changes in stratification, vertical mixing and associated biological activities. SST is well measured as a satellite product and has been identified as undergoing significant changes in recent decades, and is projected to continue evolving in response to a warming climate. A recent analysis of changes in the hydrological cycle between 1950 and 2000 [*Durack and Wijffels*, 2010, and references therein] supports a view that the water budget has also undergone significant changes in both hemispheres. Based on climate models studies these changes have been projected to increase with the future acceleration of the hydrological cycle [e.g., *Held and Soden*, 2006].

[65] Given the short length of the time series and the uncertainty implicit in our calculated oceanic pCO_2 growth rate, it is not possible to confidently separate climate variability and change based on oceanic pCO_2 measurements alone. While a more robust statistical test of the significance of growth rates would have been optimal [e.g., *Le Quéré et al.*, 2010], given the short length of the coherent time series and implicit variability such an analysis was not possible. Consequently, while the growth rates captured in this paper are at the limit of the detection, this study presents a methodology to understand the evolution of the oceanic pCO_2 growth rates and its drivers.

[66] Key to detecting and understanding how the oceanic CO_2 sink evolves in the future is a sustained longer-term CO_2 observational program. A well-designed sampling strategy [*Monteiro et al.*, 2010] should allow the attribution of observed changes in oceanic pCO_2 growth rate to climate variability and change. Additionally concomitant measurements of surface DIC and ALK are essential to an improved understanding of the drivers of the changes in the ocean carbon sink.

[67] **Acknowledgments.** A.L., B.T. and R. J. M. acknowledge support from the Australian Climate Change Science Project. N.M., T.R. and A.L. acknowledge support from the European FP6 and FP7 projects CarboOcean (contract 511176 GOCE) and CarboChange (contract 264879). N.M. also acknowledges the French national program LEFE a component of SOLAS-France. T.T and S.C.S. acknowledge support from United States NOAA grant NA080AR43207 and NSF grant ANT06-36879. M.K. acknowledges support from Pacific Climate Change Science Program.

References

Bates, N. (2001), Interannual variability of oceanic CO_2 and biogeochemical properties in the western North Atlantic subtropical gyre, *Deep Sea Res., Part II*, *48*, 1507–1528, doi:10.1016/S0967-0645(00)00151-X.

Bates, N. R. (2007), Interannual variability of the oceanic CO_2 sink in the subtropical gyre of the North Atlantic Ocean over the last 2 decades, *J. Geophys. Res.*, *112*, C09013, doi:10.1029/2006JC003759.

Behrenfeld, M. J., R. T. O'Malley, D. A. Siegel, C. R. McClain, J. L. Sarmiento, G. C. Feldman, A. J. Milligan, P. G. Falkowski, R. M. Letelier, and E. S. Boss (2006), Climate-driven trends in contemporary ocean productivity, *Nature*, *444*, 752–755, doi:10.1038/nature05317.

Bopp, L., P. Monfray, O. Aumont, J. L. Dufresne, H. Le Treut, G. Madec, L. Terray, and J. C. Orr (2001), Potential impact of climate change on marine export production, *Global Biogeochem. Cycles*, *15*, 81–99, doi:10.1029/1999GB001256.

Chen, C. T., and A. V. Borges (2009), Reconciling opposing views on carbon cycling in the coastal ocean: Continental shelves as sinks and near shore ecosystems as sources of atmospheric CO_2, *Deep Sea Res., Part II*, *56*, 578–590, doi:10.1016/j.dsr2.2009.01.001.

Chen, C. T., and F. J. Millero (1979), Gradual increase of oceanic CO_2, *Nature*, *277*, 205–206, doi:10.1038/277205a0.

Corbière, A., N. Metzl, G. Reverdin, C. Brunet, and T. Takahashi (2007), Interannual and decadal variability of the oceanic carbon sink in the North Atlantic subpolar gyre, *Tellus, Ser. B*, *59*, 168–178, doi:10.1111/j.1600-0889.2006.00232.x.

Dickson, A. G., and F. J. Millero (1987), A comparison of the equilibrium constants for the dissociation of carbonic acid in seawater media, *Deep Sea Res., Part I*, *34*, 1733–1743, doi:10.1016/0198-0149(87)90021-5.

Dong, S., J. Sprintall, S. T. Gille, and L. Talley (2008), Southern Ocean mixed-layer depth from Argo float profiles, *J. Geophys. Res.*, *113*, C06013, doi:10.1029/2006JC004051.

Dore, J. E., R. Lukas, D. W. Sadler, and D. M. Karl (2003), Climate-driven changes to the atmospheric CO_2 sink in the subtropical North Pacific Ocean, *Nature*, *424*, 754–757, doi:10.1038/nature01885.

Durack, P. J., and S. E. Wijffels (2010), Fifty-year trends in global ocean salinities and their relationship to broad-scale warming, *J. Clim.*, *23*, 4342–4362, doi:10.1175/2010JCLI3377.1.

Earth System Research Laboratory (2009), Cooperative Atmospheric Data Integration Project—Carbon Dioxide [CD-ROM], NOAA, Boulder, Colo. [Available at ftp.cmdl.noaa.gov/ccg/co2/GLOBALVIEW]

Feely, R. A., et al. (2002), Seasonal and interannual variability of CO_2 in the equatorial Pacific, *Deep Sea Res., Part II*, *49*, 2443–2469, doi:10.1016/S0967-0645(02)00044-9.

Feely, R. A., Y. Nojiri, A. J. Dickson, C. L. Sabine, M. F. Lamb, and T. Ono (2003), CO_2 in the North Pacific, Inst. of Ocean Sci., Sidney, B. C., Canada.

Feely, R. A., T. Takahashi, R. Wanninkhof, M. J. McPhaden, C. E. Cosca, S. C. Sutherland, and M. E. Carr (2006), Decadal variability of the air-sea CO_2 fluxes in the equatorial Pacific Ocean, *J. Geophys. Res.*, *111*, C08S90, doi:10.1029/2005JC003129.

Gregg, W. W., N. W. Casey, and C. R. McClain (2005), Recent trends in global ocean chlorophyll, *Geophys. Res. Lett.*, *32*, L03606, doi:10.1029/2004GL021808.

Gruber, N. (2009), Carbon cycle: Fickle trends in the ocean, *Nature*, *458*, 155–156, doi:10.1038/458155a.

Gruber, N., C. D. Keeling, and N. R. Bates (2002), Interannual variability in the North Atlantic Ocean carbon sink, *Science*, *298*, 2374–2378.

Held, I. M., and B. J. Soden (2006), Robust responses of the hydrological cycle to global warming, *J. Clim.*, *19*, 5686–5699, doi:10.1175/JCLI3990.1.

Inoue, H. Y., H. Matsuda, M. Ishii, K. Fushimi, I. Hirota, and Y. Takasugi (1995), Long-term trend of the partial pressure of carbon dioxide (pCO_2) waters of the western North Pacific, 1984–1993, *Tellus, Ser. B*, *47*, 391–413, doi:10.1034/j.1600-0889.47.issue4.2.x.

Ishii, M., et al. (2009), Spatial variability and decadal trend of the oceanic CO_2 in the western equatorial Pacific warm/fresh water, *Deep Sea Res., Part II*, *56*, 591–606, doi:10.1016/j.dsr2.2009.01.002.

Keeling, C. D., H. Brix, and N. Gruber (2004), Seasonal and long-term dynamics of the upper ocean carbon cycle at Station ALOHA near Hawaii, *Global Biogeochem. Cycles*, *18*, GB4006, doi:10.1029/2004GB002227.

Key, R. M., A. Kozyr, C. L. Sabine, K. Lee, R. Wanninkhof, J. Bullister, R. A. Feely, F. Millero, C. Mordy, and T.-H. Peng (2004), Global ocean carbon climatology: Results from Global Data Analysis Project (GLODAP), *Global Biogeochem. Cycles*, *18*, GB4031, doi:10.1029/2004GB002247.

Key, R. M., et al. (2010), The CARINA data synthesis project: Introduction and overview, *Earth Syst. Sci. Data*, *2*, 105–121, doi:10.5194/essd-2-105-2010.

Lee, K., L. T. Tong, F. J. Millero, C. L. Sabine, A. G. Dickson, C. Goyet, G. H. Park, R. Wanninkhof, R. A. Feely, and R. M. Key (2006), Global relationships of total alkalinity with salinity and temperature in surface waters of the world's oceans, *Geophys. Res. Lett.*, *33*, L19605, doi:10.1029/2006GL027207.

Lenton, A., and R. J. Matear (2007), Role of the Southern Annular Mode (SAM) in Southern Ocean CO_2 uptake, *Global Biogeochem. Cycles*, *21*, GB2016, doi:10.1029/2006GB002714.

Lenton, A., R. J. Matear, and B. Tilbrook (2006), Design of an observational strategy for quantifying the Southern Ocean uptake of CO_2, *Global Biogeochem. Cycles*, *20*, GB4010, doi:10.1029/2005GB002620.

Lenton, A., L. Bopp, and R. J. Matear (2009a), Strategies for high-latitude northern hemisphere CO_2 sampling now and in the future, *Deep Sea Res., Part II*, *56*, 523–532, doi:10.1016/j.dsr2.2008.12.008.

Lenton, A., F. Codron, L. Bopp, N. Metzl, P. Cadule, A. Tagliabue, and J. Le Sommer (2009b), Stratospheric ozone depletion reduces ocean carbon uptake and enhances ocean acidification, *Geophys. Res. Lett.*, *36*, L12606, doi:10.1029/2009GL038227.

Le Quéré, C., et al. (2007), Saturation of the Southern Ocean CO_2 sink due to recent climate change, *Science*, *316*, 1735–1738, doi:10.1126/science.1136188.

Le Quéré, C., T. Takahashi, E. Buitenhuis, C. Rodenbeck, and S. C. Sutherland (2010), Impact of climate change and variability on the global oceanic sink of CO_2, *Global Biogeochem. Cycles*, *24*, GB4007, doi:10.1029/2009GB003599.

Li, Z., D. Adamec, T. Takahashi, and S. C. Sutherland (2005), Global autocorrelation scales of the partial pressure of oceanic CO_2, *J. Geophys. Res.*, *110*, C08002, doi:10.1029/2004JC002723.

Lovenduski, N. S., and N. Gruber (2005), Impact of the Southern Annular Mode on Southern Ocean circulation and biology, *Geophys. Res. Lett.*, *32*, L11603, doi:10.1029/2005GL022727.

Lovenduski, N., N. Gruber, S. C. Doney, and I. D. Lima (2007), Enhanced CO_2 outgassing in the Southern Ocean from a positive phase of the Southern Annular Mode, *Global Biogeochem. Cycles*, *21*, GB2026, doi:10.1029/2006GB002900.

Lueker, T. J., A. G. Dickson, and C. D. Keeling (2000), Ocean pCO_2 calculated from dissolved inorganic carbon, alkalinity, and equations for K_1 and K_2: Validation based on laboratory measurements of CO_2 in gas and seawater at equilibrium, *Mar. Chem.*, *70*, 105–119, doi:10.1016/S0304-4203(00)00022-0.

Mahadevan, A., M. Lévy, and L. Mémery (2004), Mesoscale variability of sea surface pCO_2: What does it respond to?, *Global Biogeochem. Cycles*, *18*, GB1017, doi:10.1029/2003GB002102.

McKinley, G. A., A. R. Fay, T. Takahashi, and N. Metzl (2011), Convergence of atmospheric and North Atlantic carbon dioxide trends on multidecadal timescales, *Nat. Geosci.*, *4*, 606–610, doi:10.1038/ngeo1193.

Mehrbach, C., C. H. Culberson, J. E. Hawley, and R. M. Pytkowicz (1973), Measurement of the apparent dissociation constants of carbonic acid in seawater at atmospheric pressure, *Limnol. Oceanogr.*, *18*, 897–907, doi:10.4319/lo.1973.18.6.0897.

Metzl, N. (2009), Decadal increase of oceanic carbon dioxide in southern Indian Ocean surface waters (1991–2007), *Deep Sea Res., Part II*, *56*, 607–619, doi:10.1016/j.dsr2.2008.12.007.

Metzl, N., C. Brunet, A. Jabaud-Jan, A. Poisson, and B. Schauer (2006), Summer and winter air-sea CO_2 fluxes in the Southern Ocean, *Deep Sea Res., Part II*, *53*, 1548–1563.

Metzl, N., et al. (2010), Recent acceleration of the sea surface fCO_2 growth rate in the North Atlantic subpolar gyre (1993–2008) revealed by winter observations, *Global Biogeochem. Cycles*, *24*, GB4004, doi:10.1029/2009GB003658.

Midorikawa, T., K. Nemoto, H. Kamiya, M. Ishii, and H. Y. Inoue (2005), Persistently strong oceanic CO_2 sink in the western subtropical North Pacific, *Geophys. Res. Lett.*, *32*, L05612, doi:10.1029/2004GL021952.

Millero, F. J., R. H. Bryne, R. Wanninkhof, R. A. Feely, T. Clayton, P. Murphy, and M. F. Lamb (1993), The internal consistency of CO_2 measurements in the equatorial Pacific, *Mar. Chem.*, *44*, 269–280, doi:10.1016/0304-4203(93)90208-6.

Monteiro, P., et al. (2010), A global sea surface carbon observing system: Assessment of changing sea surface CO_2 and air-sea CO_2 fluxes, in *Proceedings of the OceanObs'09: Sustained Ocean Observations and Information for Society Conference, Venice, Italy, 21–25 September 2009*, edited by J. Hall, D. E. Harrison, and D. Stammer, *ESA Publ.*, *WPP-306*, Eur. Space Agency, Paris, doi:10.5270/OceanObs09.cwp.64.

Omar, A. M., and A. Olsen (2006), Reconstructing the time history of the air-sea CO_2 disequilibrium and its rate of change in the eastern subpolar North Atlantic, 1972–1989, *Geophys. Res. Lett.*, *33*, L04602, doi:10.1029/2005GL025425.

Polovina, J. J., E. A. Howell, and M. Abecassis (2008), Ocean's least productive waters are expanding, *Geophys. Res. Lett.*, *35*, L03618, doi:10.1029/2007GL031745.

Raupach, M., G. Marland, P. Cias, C. Le Quéré, J. G. Canadell, G. Klepper, and C. B. Field (2007), Global and regional drivers of accelerating CO_2 emissions, *Proc. Natl. Acad. Sci. U. S. A.*, *104*, 10,288–10,293, doi:10.1073/pnas.0700609104.

Reynolds, R. W., N. A. Rayner, T. M. Smith, D. C. Stokes, and W. Wang (2002), An improved in situ and satellite SST analysis for climate, *J. Clim.*, *15*, 1609–1625, doi:10.1175/1520-0442(2002)015<1609:AIISAS>2.0.CO;2.

Sabine, C. L., et al. (2004a), The oceanic sink for anthropogenic CO_2, *Science*, *305*, 367–371, doi:10.1126/science.1097403.

Sabine, C. L., R. A. Feely, Y. W. Watanabe, and M. Lamb (2004b), Temporal evolution of the North Pacific CO_2 uptake rate, *J. Oceanogr.*, *60*, 5–15, doi:10.1023/B:JOCE.0000038315.23875.ae.

Sabine, C. L., R. M. Key, A. Kozyr, R. A. Feely, R. Wanninkhof, F. J. Millero, T.-S. Peng, J. L. Bullister, and K. Lee (2005), Global Ocean Data Analysis Project (GLODAP): Results and data, *Rep. NDP-083*, Carbon Dioxide Inf. Anal. Cent., Oak Ridge Natl. Lab., Oak Ridge, Tenn.

Sabine, C. L., R. A. Feely, F. J. Millero, A. G. Dickson, C. Langdon, S. Mecking, and D. Greeley (2008), Decadal changes in Pacific carbon, *J. Geophys. Res.*, *113*, C07021, doi:10.1029/2007JC004577.

Santana-Casiano, J. M., M. González-Dávila, M.-J. Rueda, O. Llinás, and E.-F. González-Dávila (2007), Interannual variability of oceanic CO_2 parameters in the northeast Atlantic subtropical gyre at the ESTOC site, *Global Biogeochem. Cycles*, *21*, GB1015, doi:10.1029/2006GB002788.

Sarmiento, J. L., and N. Gruber (2006), *Ocean Biogeochemical Dynamics*, Princeton Univ. Press, Princeton, N. J.

Schuster, U., A. J. Watson, N. R. Bates, A. Corbiere, M. Gonzalez-Davila, N. Metzl, D. Pierrot, and M. Santana-Casiano (2009), Trends in North Atlantic sea-surface fCO_2 from 1990 to 2006, *Deep Sea Res., Part II*, *56*, 620–629, doi:10.1016/j.dsr2.2008.12.011.

Takahashi, T., and C. Sweeney (2002), Errors in sea-air CO_2 flux due to time-space ocean sampling strategies for sea-air pCO_2 difference, in *A Large-Scale CO_2 Observing Plan: In Situ Oceans and Atmosphere (LSCOP)*, pp. 177–183, NOAA Off. of Global Programs, Washington, D. C.

Takahashi, T., J. Olafsson, J. G. Goddard, D. W. Chipman, and S. C. Sutherland (1993), Seasonal variation of CO_2 and nutrients in the high-latitude surface oceans: A comparative study, *Global Biogeochem. Cycles*, *7*, 843–878, doi:10.1029/93GB02263.

Takahashi, T., R. A. Feely, R. F. Weiss, R. H. Wanninkhof, D. W. Chipman, S. C. Sutherland, and T. T. Takahashi (1997), Global air-sea flux of CO_2: An estimate based on measurements of sea-air pCO_2 difference, *Proc. Natl. Acad. Sci. U. S. A.*, *94*, 8292–8299, doi:10.1073/pnas.94.16.8292.

Takahashi, T., S. C. Sutherland, R. A. Feely, and R. Wanninkhof (2006), Decadal change of the surface water pCO_2 in the North Pacific: A synthesis of 35 years of observations, *J. Geophys. Res.*, *111*, C07S05, doi:10.1029/2005JC003074.

Takahashi, T., et al. (2009), Climatological mean and decadal change in surface ocean pCO_2, and net sea-air CO_2 flux over the global oceans, *Deep Sea Res., Part II*, *56*, 554–577, doi:10.1016/j.dsr2.2008.12.009.

Thomas, H., A. E. F. Prowe, I. D. Lima, S. C. Doney, R. Wanninkhof, R. J. Greatbatch, U. Schuster, and A. Corbiere (2008), Changes in the North Atlantic Oscillation influence CO_2 uptake in the North Atlantic over the past 2 decades, *Global Biogeochem. Cycles*, *22*, GB4027, doi:10.1029/2007GB003167.

Ullman, D. J., G. A. McKinley, V. Bennington, and S. Dutkiewicz (2009), Trends in the North Atlantic carbon sink: 1992–2006, *Global Biogeochem. Cycles*, *23*, GB4011, doi:10.1029/2008GB003383.

Wilks, D. S. (2006), *Statistical Methods in the Atmospheric Sciences*, 627 pp., Elsevier, Amsterdam.